INSTITUTE OF PHYSICS PUBLISHING JOURNAL OF PHYSICS B: ATOMIC, MOLECULAR AND OPTICAL PHYSICS

J. Phys. B: At. Mol. Opt. Phys. **37** (2004) 4681–4691 PII: S0953-4075(04)85628-1

Measurements of differential cross sections for elastic electron scattering in the backward direction by molecular oxygen

Ireneusz Linert[1], George C King[2] and Mariusz Zubek[1]

[1] Department of Physics of Electronic Phenomena, Gdansk University of Technology, 80-952 Gdansk, Poland
[2] Department of Physics and Astronomy, Schuster Laboratory, Manchester University, Manchester M13 9PL, UK

Received 30 August 2004
Published 22 November 2004
Online at stacks.iop.org/JPhysB/37/4681
doi:10.1088/0953-4075/37/23/009

Abstract

Absolute differential cross sections have been measured for elastic electron scattering by molecular oxygen in the backward direction over the scattering-angle range 100°–180°, at selected incident energies in the range 7–20 eV. These measurements employed the magnetic angle-changing technique with a newly designed conical-solenoid source for the localized magnetic field. The measured differential cross sections are presented together with previous experimental work and the results of theoretical calculations. Integrated elastic and momentum transfer cross sections have been deduced using the measured differential cross sections for backward scattering together with existing differential cross sections for forward scattering.

1. Introduction

Elastic electron scattering by atoms and molecules into the backward direction (scattering-angle range 90°–180°) is to a great extent governed by the short-range correlation–polarization interaction. It has been shown recently in the cases of the noble gas atoms argon (Mielewska *et al* 2004) and krypton (Cho *et al* 2004) that there exist large discrepancies between the calculated elastic differential cross sections from various theoretical approaches and the measured cross sections for backward scattering, in the low-energy region, $\leqslant$15 eV. These discrepancies are particularly striking in the angular region close to 180° and appear as significant overestimations of the calculated differential cross sections compared to the experimental ones. It has been suggested (Mielewska *et al* 2004) that these discrepancies result from the crude estimation of the correlation–polarization interaction in these calculations. Moreover, the recent calculations of McEachran and Stauffer (2003) performed in krypton over a wide energy range, 20–200 eV, show that the inclusion of absorption (inelastic channels)

lowers significantly the calculated differential cross sections for backward scattering; these calculations were based upon the relativistic polarized-orbital approximation and included static and dynamic polarization potentials. These results were also in much better agreement with experiment than the previous calculations in the angular region below 130°, where experimental cross sections are more readily available for comparison with theory.

To acquire further physical insight into backward electron scattering it is interesting to turn attention to targets with various distributions of electron density such as molecular targets, since these lead to different forms of electron–target interaction. Correlation–polarization effects are expected to be important for molecular targets and absorption effects appear at lower incident electron energies. To this end we have selected molecular oxygen as the subject of the present study. This is a diatomic homonuclear molecule with an electron–target interaction potential that is non-spherical. We have also chosen molecular oxygen because of its important role in plasmas and in the Earth's atmosphere. Moreover, several theoretical calculations have recently been published predicting differential cross sections for backward scattering in molecular oxygen with which the present measurements can be compared. The present measurements also allow the integral cross section for elastic scattering and momentum transfer cross section to be determined with higher accuracy than was previously possible. This is because previous determinations depended upon extrapolation procedures over a wide angular range to estimate the differential cross section in the backward-scattering direction which here is measured directly.

The first differential cross section measurements in molecular oxygen, in the low-energy range, were performed by Trajmar *et al* (1971), from 4 eV to 45 eV, and by Linder and Schmidt (1971), in the region below 4 eV. These measurements were limited to the scattering-angle ranges of 10°–90° and 20°–110° respectively which correspond mainly to the range of forward scattering. Measurements over an extended scattering-angle range, also using conventional electron spectrometers, were subsequently carried out by Dehmel *et al* (1976) up to 150° at electron energies of 5 eV and 15 eV, by Wakiya (1978) in the range 10°–130° and in the higher energy region from 20 eV to 500 eV and by Shyn and Sharp (1982) up to 156° in the energy range 2 eV to 200 eV. In the studies of Dehmel *et al* and Wakiya the absolute values of the differential cross sections were deduced by extrapolating their measured cross sections down to 0° and up to 180° and then normalizing the resulting integrated cross sections to the known total cross sections. Shyn and Sharp, on the other hand, used a static gas method and normalized their cross sections against those of helium. The differential cross sections of Shyn and Sharp served as calibration points for the more recent measurements of low-energy elastic cross sections by Middleton *et al* (1994) and Woeste *et al* (1995), both performed over the angular range 10°–90°. Sullivan *et al* (1995) were the first to use the relative flow technique to obtain absolute differential cross sections in molecular oxygen. They employed helium as a reference standard and used electron energies below 30 eV and the range of scattering angles from 10° to 130°. The most recent measurements, by Green *et al* (1997) who also employed the relative flow technique, were aimed at resolving the discrepancies that existed in the measured differential cross sections at scattering angles below 60° in the energy region from 5 eV to 10 eV. The results of Green *et al* supported those of Sullivan *et al*. Further discussion of the above experimental works can be found in the comprehensive review of scattering cross sections for diatomic molecules by Brunger and Buckman (2002).

In the present work, we have measured for the first time the absolute differential cross sections for elastic electron scattering in molecular oxygen in the scattering-angle range from 100° to 180°. We have done this for incident electron energies in the range from 7 eV to 20 eV. In these measurements, the angle-changing technique (Zubek *et al* 1999, Linert *et al* 2004) has been used to observe scattering in the backward direction and the relative flow technique

has been used to place the cross sections on an absolute scale. Our results are in very good agreement with those of Sullivan *et al* (1995) in the angular range from 100° to 130° where the measurements overlap, but extend significantly the angular range of previous measurements.

There are three recent theoretical calculations that predict the elastic differential cross sections over the whole scattering-angle range 0°–180° and can be compared with the present measurements. Nordbeck *et al* (1994) and Woeste *et al* (1995) used the *R*-matrix method and included nine target states that were represented by the configuration-interaction wavefunctions of Noble and Burke (1992). In these calculations, the short-range polarization interaction was accounted for by a second term in the total wavefunction which involved summation over a number of electron–target wavefunctions. A Schwinger multichannel approach that included the first three inelastic electronic channels of oxygen was applied by da Paixao *et al* (1992) in their static-exchange calculations (Lima *et al* 1990). In the third and most recent approach Machado *et al* (1999) combined the Schwinger method and the distorted-wave approximation to calculate elastic electron scattering in the energy range from 5 eV to 500 eV. Here, the electron–target interaction was described by a complex optical potential. This potential included absorption effects as well as static, exchange and correlation–polarization contributions, the last one in the framework of the free-electron-gas model.

2. Experimental apparatus and procedures

The measurements of the differential cross sections were performed with an electrostatic electron spectrometer that has been equipped with a new conical-solenoid system for the implementation of the magnetic angle-changing technique. The electron spectrometer has been described in detail previously by Zubek and King (1994). Briefly, it consists of an electron monochromator and an electron energy analyser which can be rotated through the angular range −10°–120° with respect to the direction of the incident electron beam. The electron beam leaving the hemispherical deflector of the monochromator is focused onto the molecular gas beam by a combination of two triple-aperture lenses. Electrons scattered off the molecular beam are focused onto the entrance slit of the hemispherical deflector of the electron analyser by a three-element cylinder lens. A channel electron multiplier is used to detect electrons transmitted by the analyser. The overall energy resolution of the spectrometer in the present measurements was approximately 60 meV.

The new conical-solenoid system has been described in detail by Linert *et al* (2004). It produces a localized, static magnetic field at the interaction region of the spectrometer. This magnetic field deflects the incident and scattered electrons in such a way that backward-scattering angles up to 180° can be reached. The solenoid system is shown schematically in figure 1 and consists of two pairs of conical coils, namely an inner pair and an outer pair. The axis of cylindrical symmetry of the solenoids is perpendicular to the scattering plane. Each inner-coil contains six layers of wire and each outer-coil contains four layers. The number of turns in the layers increases from 1 to 6 in the inner-coils and from 7 to 10 in the outer-coils. The conical shape of the coils satisfies the geometrical condition given by Read and Channing (1996) required to obtain an octupole moment of the magnetic system equal to zero. The ratio of currents in the inner and outer-coils, 1:−0.327, is chosen to obtain the magnetic dipole moment of the system also equal to zero; the quadrupole and 16-pole magnetic moments of any current-carrying system with cylindrical symmetry are automatically zero. These properties of the solenoid system produce a very rapid decrease of the resultant magnetic field with radial distance which ensures that the performances of the monochromator and electron analyser of the spectrometer are not affected adversely. A further advantage of this conical geometry is

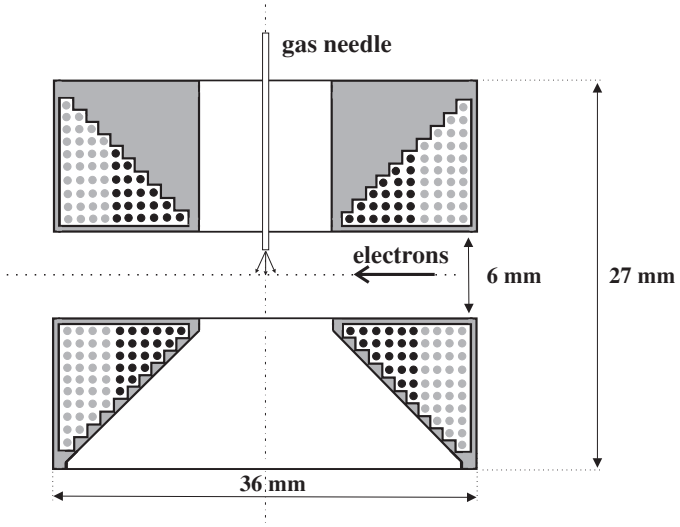

Figure 1. Schematic diagram of the conical-solenoid system that produces the localized magnetic field at the interaction region. Inner-coils and outer-coils are indicated by full black and full grey circles, respectively.

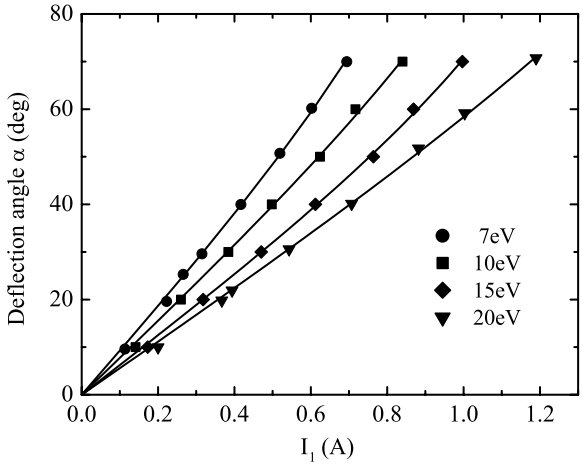

Figure 2. Measured total deflection angle α for electrons of the indicated energy as a function of the inner-coil current I_1 of the conical-solenoid system.

that it has an open structure (figure 1) so that the target gas is efficiently pumped away from the interaction region.

The total deflection angle α of electrons of a given electron energy E depends on the currents flowing in the coils and can be conveniently expressed in terms of the inner-coil current I_1. The dependence of α on I_1 has been measured for each electron energy studied in this work, i.e. 7, 10, 15 and 20 eV by measuring the total deflection angle of the unscattered primary beam for various values of I_1. The resultant curves are shown in figure 2. They have been approximated by an analytical expression (Read and Channing 1996) of the form

$$\alpha = a \arcsin\left(\frac{cI_1}{\sqrt{E}}\right) \tag{1}$$

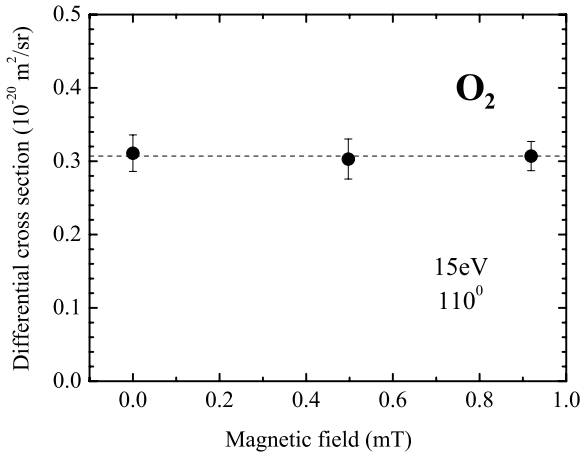

Figure 3. Measured values of the differential cross section of molecular oxygen for an incident electron energy of 15 eV and a scattering angle of 110° obtained at three different values of the deflecting magnetic field.

where a and c are constants. Equation (1) shows how I_1 (and in turn the outer-coil current) has to be adjusted to obtain a particular value of deflection angle for a particular value of incident electron energy. In the present measurements, the scattered electron analyser was placed at a fixed position of 110° with respect to the initial direction of the incident electron beam. Then for each value of (fixed) incident electron energy the scattering angles in the range from 120° to 180° were selected by adjusting the currents in the coils according to equation (1); the measurements at 100° and 110° were made without application of the magnetic field. The absolute scattering-angle scale was calibrated by observing the minimum in the region of 120° in the elastic scattering cross section of argon. The total uncertainty in the angular scale of the present studies is estimated to be ±2°and the angular resolution of the measurements is estimated to be 4°. To verify that the measured cross sections were independent of the magnetic field used we have performed test measurements of the differential cross section at an incident energy of 15 eV and a scattering angle of 110°. These measurements (figure 3) were obtained at three different values of the magnetic field and to maintain a fixed scattering angle of 110° the position of the electron analyser was adjusted appropriately. These three measurements deviate from their average value by less than 1% which confirms the independence of the measured differential cross sections on the magnetic field used.

This mode of operation is different from that used in our previous measurements of elastic differential cross sections, e.g. Zubek *et al* (2000). In these previous measurements we maintained the solenoid currents at constant values to produce a fixed deflection angle at a given electron energy and instead rotated the scattered electron analyser. The present mode of operation has the experimental advantage that it is more convenient to change the currents in the coil than mechanically rotating the analyser.

To obtain absolute values of the differential cross sections we have applied the relative flow technique (Srivastava *et al* 1975, Nickel *et al* 1989). We used helium as the reference gas together with the theoretical cross sections of Nesbet (1979) in the energy region 15 eV and below and of Saha (1989) at 20 eV. The experimental procedure employed to measure the relative flow rates of the oxygen and helium gases was similar to that proposed by Khakoo and Trajmar (1986). The atomic and molecular beams are formed by a single capillary having an internal diameter of 0.3 mm and a length of 10 mm. A shut-off valve is placed between

this capillary and the leak valve which is used to control the target-gas flow. This establishes a well-defined volume between these two valves. The relative gas flows for the oxygen and helium gases were determined from their measured rates of pressure increase in this volume when the shut-off valve was closed. The driving pressure of oxygen behind the capillary was maintained below 0.4 mbar and the ratio of driving pressures for oxygen to that of helium was adjusted to be 0.37 to maintain equal mean free path lengths for both gases in the beam-forming capillary, as determined from their molecular and atomic diameters (CRC 1998/1999).

High operational stability of the electron spectrometer was achieved by ensuring that oxygen and helium gases were always present simultaneously in the vacuum chamber. This was accomplished by admitting one gas to the scattering region through the capillary and the other directly to the vacuum chamber through a side valve. The measured yields of scattered electrons contain contributions from the background gas present in the interaction region. These contributions were determined by bypassing the capillary and admitting the oxygen and helium gases directly into the vacuum chamber. These background contributions have been subtracted from the measured electron yields. The electron energy was calibrated against the position of the He^-resonance at 19.37 eV to within ± 30 meV using the mixture of oxygen and helium gases.

Measurements of the differential cross section at each value of incident electron energy were repeated a number of times. These measurements had uncertainties arising from the determinations of the relative flow rates of oxygen and helium, the yields of scattered electrons and the incident electron current and also from the uncertainties in the theoretical cross sections of Nesbet (1979) and Saha (1989) for helium which from comparison with other calculations were taken to be 2% and 2.5% respectively. The resultant uncertainties in the differential cross sections quoted here were deduced from the statistical spread of the individual measurements and correspond to three standard deviations of the data. The resultant uncertainties are estimated to be 10% for the 7 and 10 eV cross sections and 8% for the 15 and 20 eV cross sections.

3. Results and discussion

3.1. Differential cross sections

Our differential cross sections, measured over the scattering-angle range from 100° to 180° for incident electron energies of 7, 10, 15 and 20 eV are presented in figures 4(a) to (d). Also presented are the experimental results of Trajmar *et al* (1971), Dehmel *et al* (1976), Shyn and Sharp (1982), Woeste *et al* (1995), Sullivan *et al* (1995) and Green *et al* (1997) which essentially cover the region of forward scattering. These figures also make a comparison of the experimental measurements with the theoretical calculations of da Paixao *et al* (1992), Nordbeck *et al* (1994), Woeste *et al* (1995) and Machado *et al* (1999) that cover the whole scattering-angle range, 0° to 180°. The present results are also listed in table 1.

At the energy of 7 eV (figure 4(a)) our cross section values at 100° and 110° coincide with those of Sullivan *et al* (1995). Our results then rise slowly with increasing angle to reach a plateau in the vicinity of 180°. This angular dependence is much weaker than that shown by the cross section of Shyn and Sharp (1982). This discrepancy may indicate a significant overestimation of the backward-scattering cross section in their measurements. The *R*-matrix calculations of Woeste *et al* (1995) are in better agreement with our results than the calculations of Machado *et al* (1999) which at 180° predict the cross section to be about 30% higher than our experimental value. It is to be noted, however, that in the angular region below 60° the results of Machado *et al* display an angular behaviour that is in much better accord with the measured

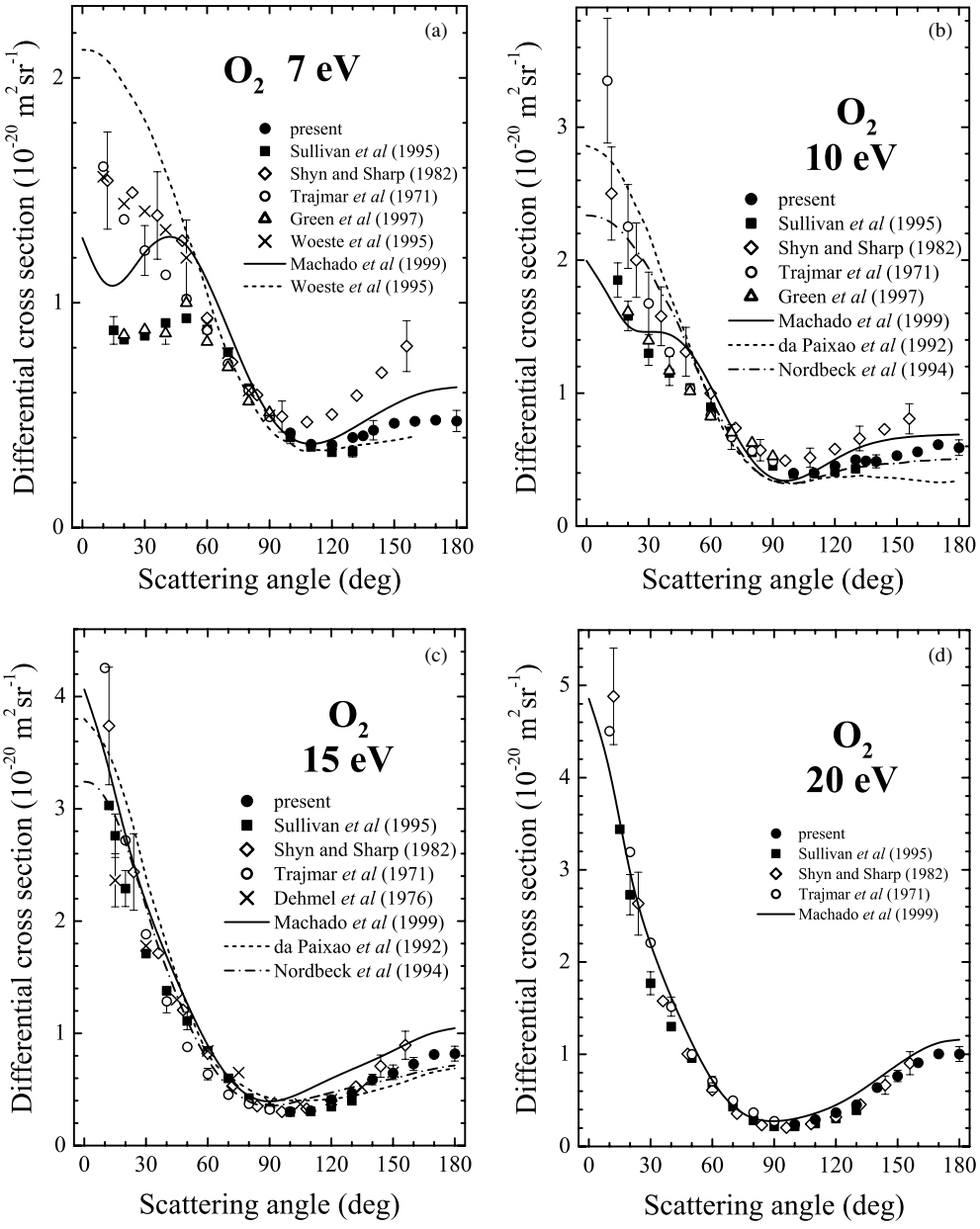

Figure 4. Absolute differential cross sections for elastic electron scattering in molecular oxygen at incident energies of (a) 7 eV, (b) 10 eV, (c) 15 eV and (d) 20 eV. The present results are shown together with previous experimental and theoretical results as indicated.

cross sections of Sullivan *et al* and Green *et al* (1997) than those of Woeste *et al*. Machado *et al* combined the Schwinger variational method and the distorted-wave approximation.

At the energy of 10 eV (figure 4(b)) our cross section values agree well with the results of Sullivan *et al* (1995) for scattering angles from 100° to 130° and then show a tendency to increase slowly with an angle above 110°. There is again a large discrepancy with respect

Table 1. Differential cross sections in units of 10^{-20} m^2 sr^{-1} for elastic electron scattering from molecular oxygen at incident energies of 7, 10, 15 and 20 eV.

Scattering angle (degree)	Energy (eV)			
	7	10	15	20
100	0.421	0.399	0.303	0.239
110	0.371	0.401	0.311	0.293
120	0.369	0.455	0.409	0.367
130	0.401	0.500	0.468	0.452
135	0.408	0.490	–	–
140	0.433	0.487	0.588	0.639
150	0.464	0.530	0.647	0.764
160	0.473	0.559	0.727	0.908
170	0.478	0.613	0.812	1.005
180	0.474	0.590	0.819	1.002

to the measurements of Shyn and Sharp (1982) in the angular range above 120°. Of the three theoretical calculations, the results of Nordbeck *et al* (1994) seem to be the closest to our experimental values. Their results were obtained from *R*-matrix calculations using the target state representation that was subsequently employed in the calculations by Woeste *et al* (1995). Of the other two theoretical works, that of Machado *et al* (1999) gives a cross section that is about 15% higher at 180° than our measurements while the cross section of da Paixao *et al* (1992) is much lower at 180° than our value. Similarly as for the incident energy of 7 eV, the results of Machado *et al* below 30° are the closest to the measurements of Sullivan *et al* (1995).

At 15 eV (figure 4(c)) our cross section increases faster with scattering angle above 100° than at lower energies. For scattering angles from 100° to 130° our measurements, as before, coincide with the measurements of Sullivan *et al* (1995), while those of Shyn and Sharp (1982) are now closer to both of these. The latter, however, tend to increase much faster with scattering angle above 130°. It is interesting to note that the early measurements of Dehmel *et al* (1976) show good agreement with our cross sections in their range of scattering angle up to 150°. The differential cross sections calculated by da Paixao *et al* (1992) and Nordbeck *et al* (1994) almost coincide with each other in the range of backward scattering and are in general agreement with our experimental cross section. The cross sections of Machado *et al* (1999), as for incident energies of 7 eV and 10 eV, appear to overestimate the scattering cross section above 110° but again are in accord with the experimental cross sections for forward scattering. The overestimation is about 20% at 180°.

At the energy of 20 eV (figure 4(d)) all the experimental cross sections, including our own, are in very good agreement with each other. This applies also to the results of Shyn and Sharp (1982). The calculated cross section of Machado *et al* (1999) lies only slightly above our results and reflects very well the angular dependence of the differential cross section over the whole angular range of the experimental investigations.

3.2. Integral elastic and momentum transfer cross sections

We have also determined integral elastic and momentum transfer cross sections for molecular oxygen by integrating the differential cross sections at each electron energy. This involved combining the present measurements for the backward-scattering range, 100°–180°, with the measurements of Sullivan *et al* (1995) for the 15°–100° range. This also involved extrapolation

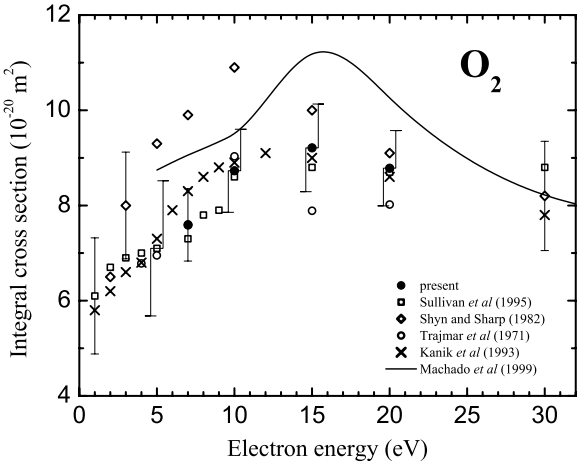

Figure 5. Integral elastic cross section of molecular oxygen. The present results are shown together with previous experimental and theoretical results as indicated.

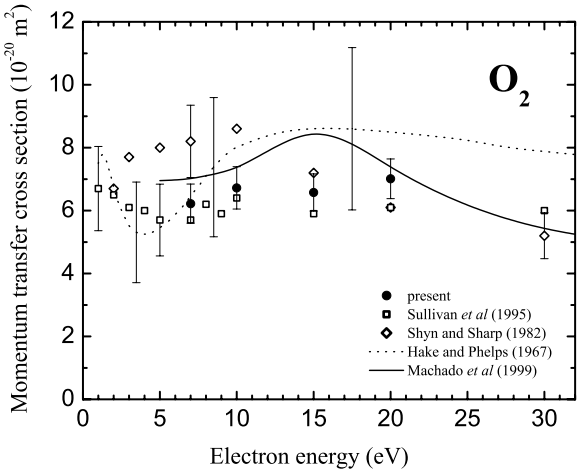

Figure 6. Momentum transfer cross section of molecular oxygen. The present results are shown together with previous experimental and theoretical results as indicated.

of the cross sections of Sullivan *et al* down to 0° using the calculated values of Machado *et al* (1999) as a guide to the angular dependence of the cross section. The integral elastic and momentum transfer cross sections obtained are shown in figures 5 and 6, respectively, and listed in table 2. We estimate the uncertainties of our cross sections to be 10% at 7 eV and 10 eV and 9% at 15 eV and 20 eV. These include the uncertainty of 7–9% quoted for the results of Sullivan *et al* and the estimated uncertainties of our differential measurements. The extrapolation procedure to obtain the integrated cross sections over the 0°–15° range contributes uncertainties of less than 0.5% to the integral elastic and momentum transfer cross sections.

Our integral elastic cross section (figure 5) has a weak maximum at about 15 eV. It is in very good agreement with the estimated cross section of Sullivan *et al* (1995) supporting their assumption concerning the behaviour of the differential cross sections in the angular

Table 2. Integral elastic Q_e and momentum transfer Q_m cross sections in units of 10^{-20} m^2 for molecular oxygen at incident energies of 7, 10, 15 and 20 eV.

	Energy (eV)			
	7	10	15	20
Q_e	7.59	8.73	9.21	8.78
Q_m	6.22	6.72	6.58	7.01

range above 130°. It is also in very good agreement with the recommended cross section of Kanik *et al* (1993) which was determined from a thorough analysis of the available total and excitation cross section data. The estimated integral cross section of Shyn and Sharp (1982), on the other hand, lies above the results of Sullivan *et al*, Kanik *et al* and the present work. We ascribe this to the higher values of the differential cross section obtained by Shyn and Sharp for backward and also forward scattering. The theoretical cross section of Machado *et al* (1999) also shows a maximum at about 15 eV in agreement with the present experimental values but lies about 20% above them. This maximum appears in the energy region of the $^4\Sigma^-$ resonance state which has been clearly observed in vibrational excitation of the oxygen molecule (Allan 1995).

Our momentum transfer cross section (figure 6) is in good accord with the results of Sullivan *et al* (1995) while the cross section of Shyn and Sharp (1982) lies noticeably above both in the energy region below 15 eV. The swarm measurements of Hake and Phelps (1967) appear to overestimate the cross section in the energy region above 7 eV but are in reasonable agreement with the results of Sullivan *et al* below that energy. The calculated cross section of Machado *et al* (1999) indicates a weak maximum at around 15 eV.

4. Conclusions

We have measured differential cross sections for elastic electron scattering in molecular oxygen over the range of scattering angles from 100° to 180° and at the electron incident energies of 7, 10, 15 and 20 eV. These are the first experimental determinations of these cross sections at and close to 180°. These backward-scattering measurements have been compared with the three available calculations of the elastic cross sections. This comparison indicates that the *R*-matrix calculations of Woeste *et al* (1995) at 7 eV and Nordbeck *et al* (1994) at 10 eV give the best agreement with the backward-scattering measurements. However, these calculations lie much above the recent measurements for forward scattering at these energies (Sullivan *et al* 1995, Green *et al* 1997). Interestingly, these features of the *R*-matrix calculations were also seen in our measurement of the elastic differential cross section in molecular nitrogen at 5 eV (Zubek *et al* 2000). There the *R*-matrix calculations of Gillan *et al* (1987) agreed well with the experimental values for backward scattering but disagreed with the values for forward scattering. This may be a general feature of the *R*-matrix approach at lower energies. At 15 eV in molecular oxygen the *R*-matrix calculations are in good agreement with experiment over the whole angular range as are the Schwinger multichannel calculations of da Paixao *et al* (1992).

We note that at incident energies below 10 eV and in the angular range close to 180°, the differences between the theoretical and the measured differential cross sections are less in the case of the small molecules, oxygen and nitrogen, than they are for the noble gas atoms, argon and krypton. This also appears to be the case for the water molecule in the energy range 6–15 eV (Cho *et al* 2004). Finally, we expect that detailed future theoretical calculations of

the differential cross sections will lead to greater physical insight into the roles played by the various types of interactions between the incident electron and the target.

References

Allan M 1995 *J. Phys. B: At. Mol. Opt. Phys.* **28** 5163
Brunger M J and Buckman S J 2002 *Phys. Rep.* **357** 215
Cho H, Gulley R J and Buckman S J 2003 *J. Korean Phys. Soc.* **42** 71
Cho H, Park Y S, Tanaka H and Buckman S J 2004 *J. Phys. B: At. Mol. Opt. Phys.* **37** 625
CRC 1998/1999 *Handbook of Chemistry and Physics* 78th edn ed D R Lide (Boca Raton, FL: CRC Press)
da Paixao F J, Lima M A P and McKoy V 1992 *Phys. Rev. Lett.* **68** 1698
Dehmel R C, Fineman M A and Miller D R 1976 *Phys. Rev.* A **13** 115
Green M A, Teubner P J O, Mojarrabi B and Brunger M J 1997 *J. Phys. B: At. Mol. Opt. Phys.* **30** 1813
Hake R D and Phelps A V 1967 *Phys. Rev.* **151** 70
Kanik I, Trajmar S and Nickel J C 1993 *J. Geophys. Res.* **98** 7447
Khakoo M A and Trajmar S 1986 *Phys. Rev.* A **34** 138
Lima M A P, Brescansin L M, da Silva A J R, Winstead C and McKoy V 1990 *Phys. Rev.* A **41** 327
Linder F and Schmidt H 1971 *Z. Naturf.* a **26** 1617
Linert I, King G C and Zubek M 2004 *J. Electron Spectrosc. Rel. Phenom.* **134** 1
Machado L E, Ribeiro E M S, Lee M-T, Fujimoto M M and Brescansin L M 1999 *Phys. Rev.* A **60** 1199
McEahran R P and Stauffer A D 2003 *J. Phys. B: At. Mol. Opt. Phys.* **36** 3977
Middleton A G, Brunger M J, Teubner P J O, Anderson M W B, Noble C J, Woste G, Blum K, Burke P G and Fullerton C 1994 *J. Phys. B: At. Mol. Opt. Phys.* **27** 4057
Mielewska B, Linert I, King G C and Zubek M 2004 *Phys. Rev.* A **69** 062716
Nesbet R K 1979 *Phys. Rev.* A **20** 58
Nickel J C, Zetner P W, Shen G and Trajmar S 1989 *J. Phys E: Sci. Instrum.* **22** 730
Noble C J and Burke P G 1992 *Phys. Rev. Lett.* **68** 2011
Nordbeck R-P, Fullerton C M, Woeste G, Thompson D G and Blum K 1994 *J. Phys. B: At. Mol. Opt. Phys.* **27** 5375
Read F H and Channing J M 1996 *Rev. Sci. Instrum.* **67** 2372
Saha H P 1989 *Phys. Rev.* A **40** 2976
Shyn T W and Sharp W E 1982 *Phys. Rev.* A **26** 1369
Srivastava S K, Chutjian A and Trajmar S 1975 *J. Chem. Phys.* **63** 2659
Sullivan J P, Gibson J C, Gulley R J and Buckman S 1995 *J. Phys. B: At. Mol. Opt. Phys.* **28** 4319
Trajmar S, Cartwright D S and Williams W 1971 *Phys. Rev.* A **4** 1482
Wakiya K 1978 *J. Phys. B: At. Mol. Phys.* **11** 3913
Woeste G, Noble C J, Higgins K, Burke P G, Brunger M J, Teubner P J O and Middleton A G 1995 *J. Phys. B: At. Mol. Opt. Phys.* **28** 4141
Zubek M and King G C 1994 *J. Phys. B: At. Mol. Opt. Phys.* **27** 2613
Zubek M, Mielewska B, Channing J M, King G C and Read F H 1999 *J. Phys. B: At. Mol. Opt. Phys.* **32** 1351
Zubek M, Mielewska B and King G C 2000 *J. Phys. B: At. Mol. Opt. Phys.* **33** L527